The XXVII International Scientific Conference of Young Scientists and Specialists

Thermal transport in aluminum oxide irradiated with swift heavy ions

<u>A.B. Akzhunussov</u>
R.A. Rymzhanov
A.E.Volkov

JOINT INSTITUTE
FOR NUCLEAR RESEARCH

НАЦИОНАЛЬНЫЙ
ИССЛЕДОВАТЕЛЬСКИЙ ЦЕНТР
"КУРЧАТОВСКИЙ
ИНСТИТУТ"

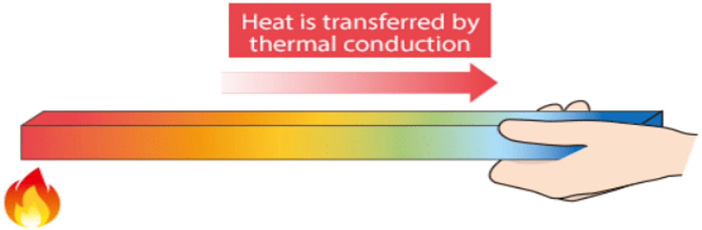

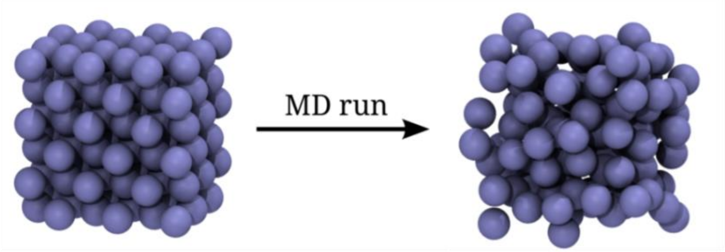

Outline

- MOTIVATION
- METHOD
- SIMULATION
- RESULT
- SUMMARY

Dubna – 2023 y.

MOTIVATION

EFFECT OF SWIFT HEAVY IONS

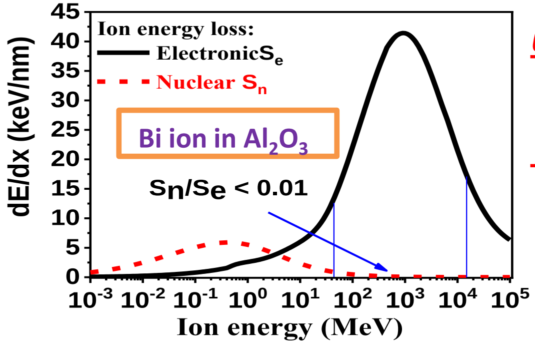

$E > 0.5$ MeV/nucl,

$M > 4m_p$

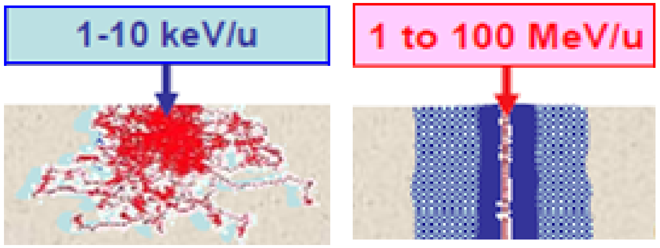

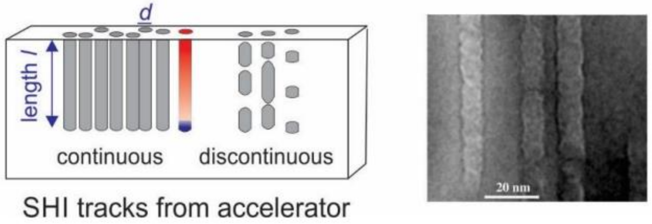

Schematic representation and TEM image of tracks

- *Simulate an influence of fission fragments and cosmic rays on material properties;*
- *Nanostructuring of solids*

THERMAL CONDUCTIVITY DEGRADATION

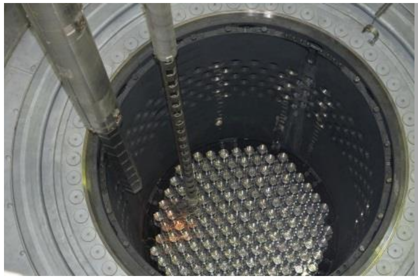

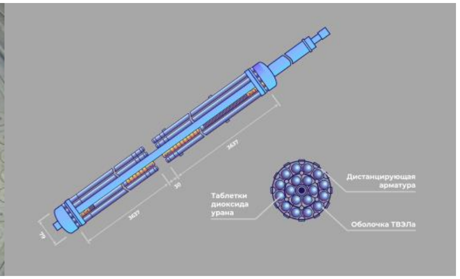

- *The resistance at irradiation with n, alpha and fission fragments;*
- *Good thermal properties*
- *The aluminum oxide (Al_2O_3) is a promising material for various nuclear applications, it is considered as a candidate material for inert matrix fuel host in the reactor core;*
- *Study thermal conductivity degradation after irradiation with fission fragments is an important issue of materials for future high temperature nuclear reactors.*

METHOD

Molecular Dynamics

http://lammps.sandia.gov/

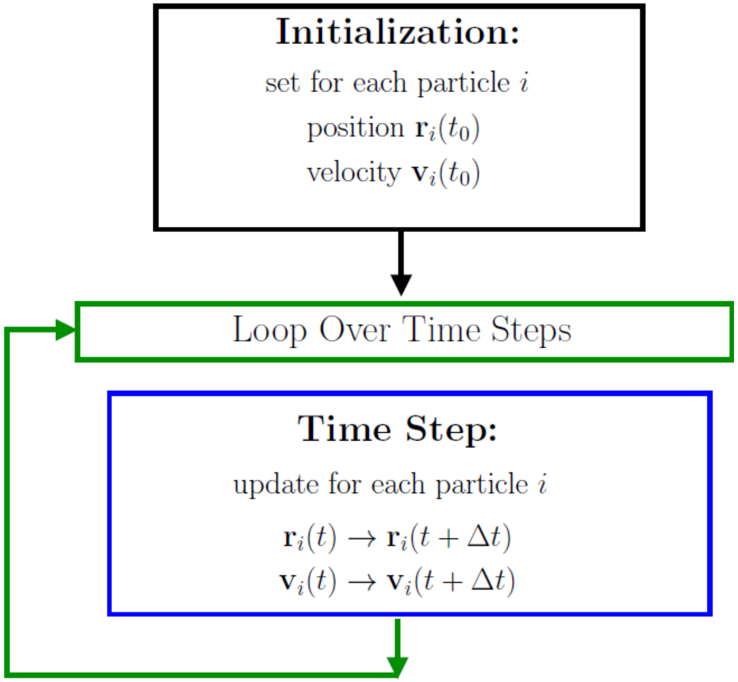

Initialization:

set for each particle i

position $\mathbf{r}_i(t_0)$

velocity $\mathbf{v}_i(t_0)$

Loop Over Time Steps

Time Step:

update for each particle i

$\mathbf{r}_i(t) \rightarrow \mathbf{r}_i(t+\Delta t)$

$\mathbf{v}_i(t) \rightarrow \mathbf{v}_i(t+\Delta t)$

MD based on solving Newton equations:

$$\boxed{\vec{F} = -\vec{\nabla} V}$$

$$\boxed{m_i \frac{d^2 r_i(t)}{dt^2} = F_i(r), i = 1,2, \dots, n.}$$

Initial conditions for simulation with MD

Crystal structure (Unit cell)

$$\rho = 3.99 \, {}^{g}/_{cm^3}$$

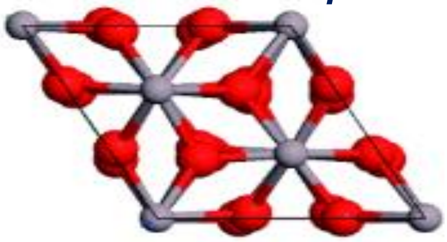

Al_2O_3 has a trigonal syngony with the space group R3c.The crystal lattice consists of Al^{3+} and O^{2-}. Oxygen ions form a distorted hexagonal dense packing, and aluminum cations occupy 2/3 of octahedral voids

Interatomic potential

$$V = \sum_{i<j} V_{ij}^{(2)}(r_{ij}) + \sum_{i,j<k} V_{jik}^{(3)}(r_{ij}, r_{ik}).$$

$$V_{ij}^{(2)}(r) = \frac{H_{ij}}{r^{\eta_{ij}}} + \frac{Z_i Z_j}{r} e^{-r/\lambda} - \frac{D_{ij}}{r^4} e^{-r/\xi} - \frac{W_{ij}}{r^6}.$$

$$V_{jik}^{(3)}(r_{ij}, r_{ik}) = R^{(3)}(r_{ij}, r_{ik}) P^{(3)}(\theta_{jik}),$$

Three-body Vashishta-type potential[1]

[1] P. Vashishta et al., J. Appl. Phys. 103 (8) (2008) 083504

SIMULATION

1) Track formation = TREKIS + MD

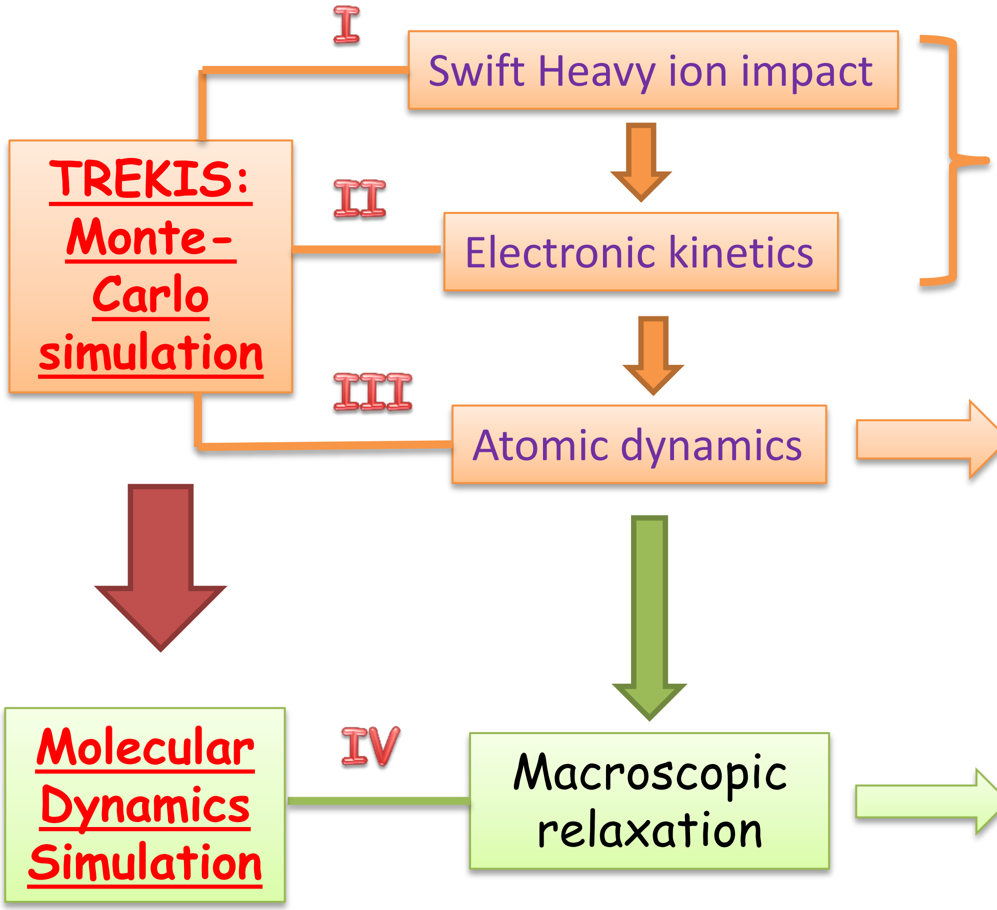

TREKIS: Monte-Carlo simulation

I Swift Heavy ion impact

II Electronic kinetics

III Atomic dynamics

Molecular Dynamics Simulation

IV Macroscopic relaxation

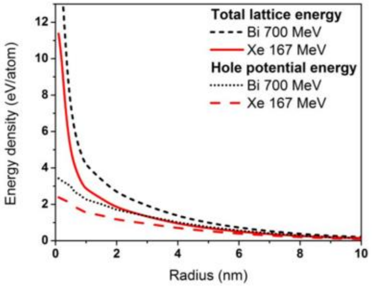

Distribution of excess lattice energy[2]

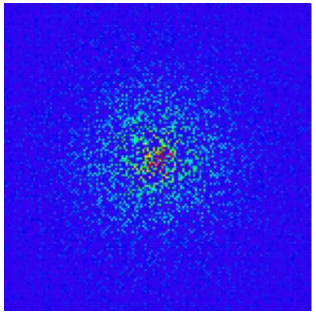

Velocity distribution of atoms

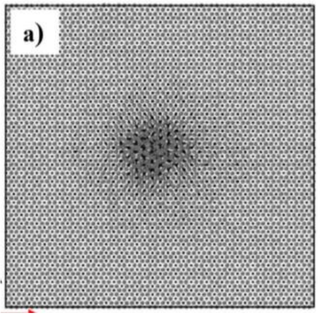

Formation track [3]

OVITO
Open Visualization Tool

https://www.ovito.org/

Further this structure was used as input data for simulation thermal conductivity

Was very successfully applied for other materials: Si_3N_4 , LiF, Y_2O_3, Olivine, CaF_2, WO_3, ZrO_2, ZnO

[2] R.A. Rymzhanov et al., J. Phys. D. Appl. Phys. 48 (2015) 355303.

[3] R. Rymzhanov et al.,, J. Phys. D. Appl. Phys. 50 (2017) 475301.

2) Direct method for calculation thermal conductivity (Fourier law)

I. Creation of non-equilibrium system

II. Transition of the system to a stationary state;
Computation of thermal conductivity.

III. We used the simulation cells varying from 29 to 330 nm (22–250 unit cells) in length.

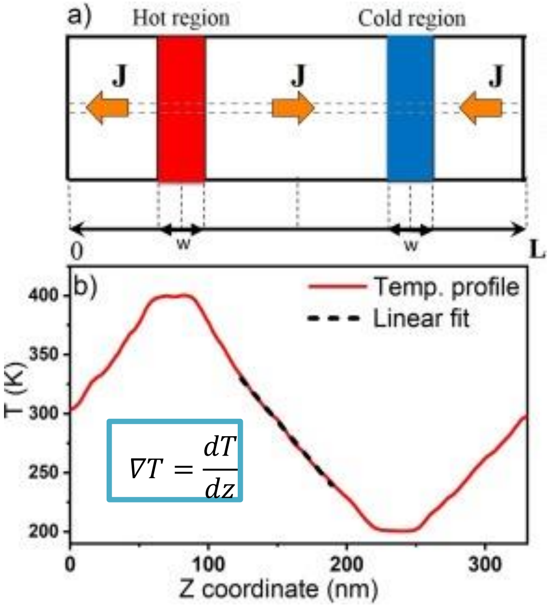

$$\nabla T = \frac{dT}{dz}$$

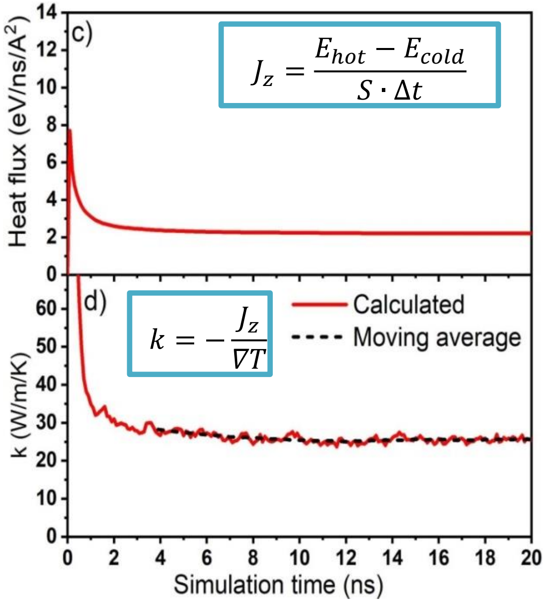

$$J_z = \frac{E_{hot} - E_{cold}}{S \cdot \Delta t}$$

$$k = -\frac{J_z}{\nabla T}$$

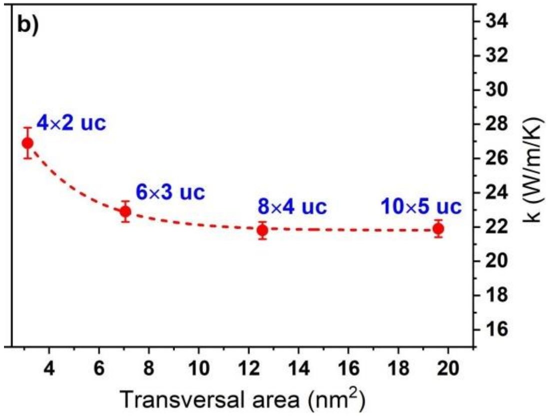

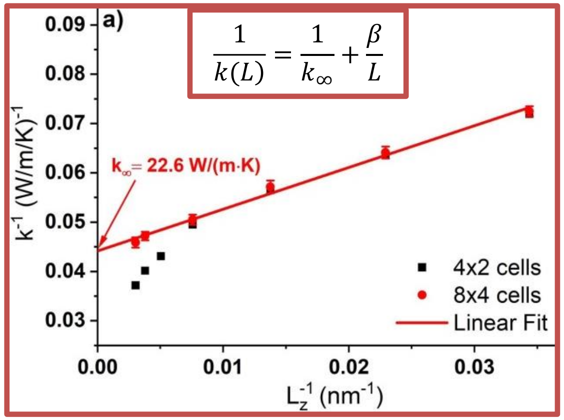

$$\frac{1}{k(L)} = \frac{1}{k_\infty} + \frac{\beta}{L}$$

This problem is solved with the well-developed method of thermal conductivity calculations in several simulation cells of different sizes with subsequent extrapolation of its value to an infinitely large system, k∞, according to the Mathiessen's rule.

RESULT

1) Change of thermal conductivity after SHI irradiation

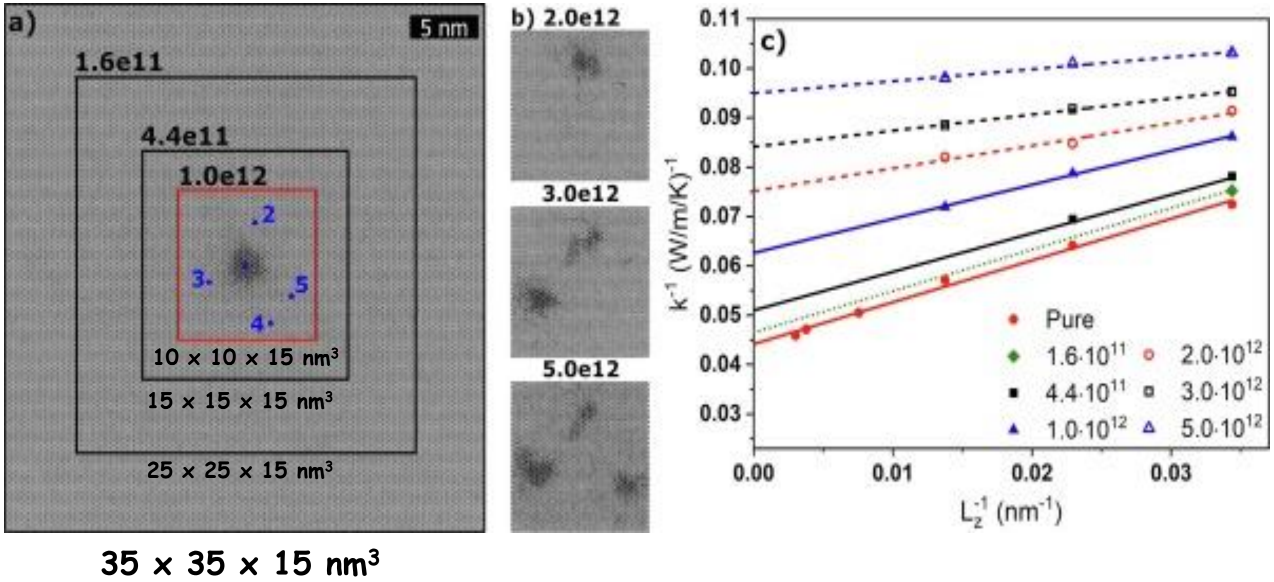

(a) MD simulated track of 167 MeV Xe ion in alumina. The squares show cut cells for different fluences. Blue dots with numbers shows the positions of the ion trajectories in order of its simulations. (b) Selected central area with simulated several subsequent ion passages. (c) Plot of inverse thermal conductivity vs inverse cell length for different fluences

$$Fluence = \frac{N}{S}$$

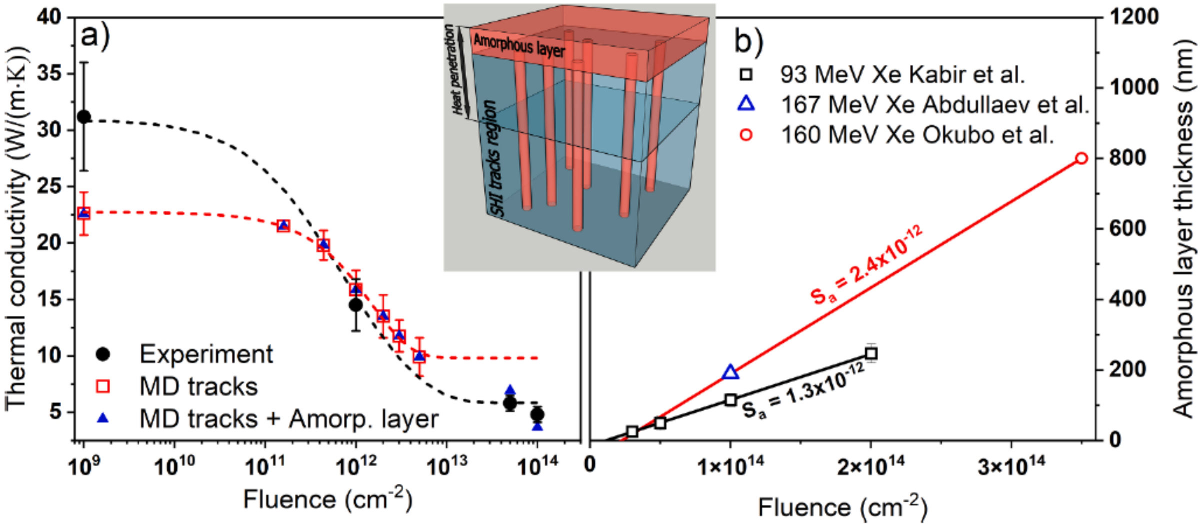

(a) Fluence dependence of the calculated thermal conductivity coefficient of alumina. Experimental data and their fit with the phonon-mediated thermal transport model. (b) Thickness of amorphous layer for Xe ions of different energies from Kabir et al., Abdullaev et al., Okubo et al.. Inset shows the scheme of layered structure of Al2O3 irradiated with high fluences.

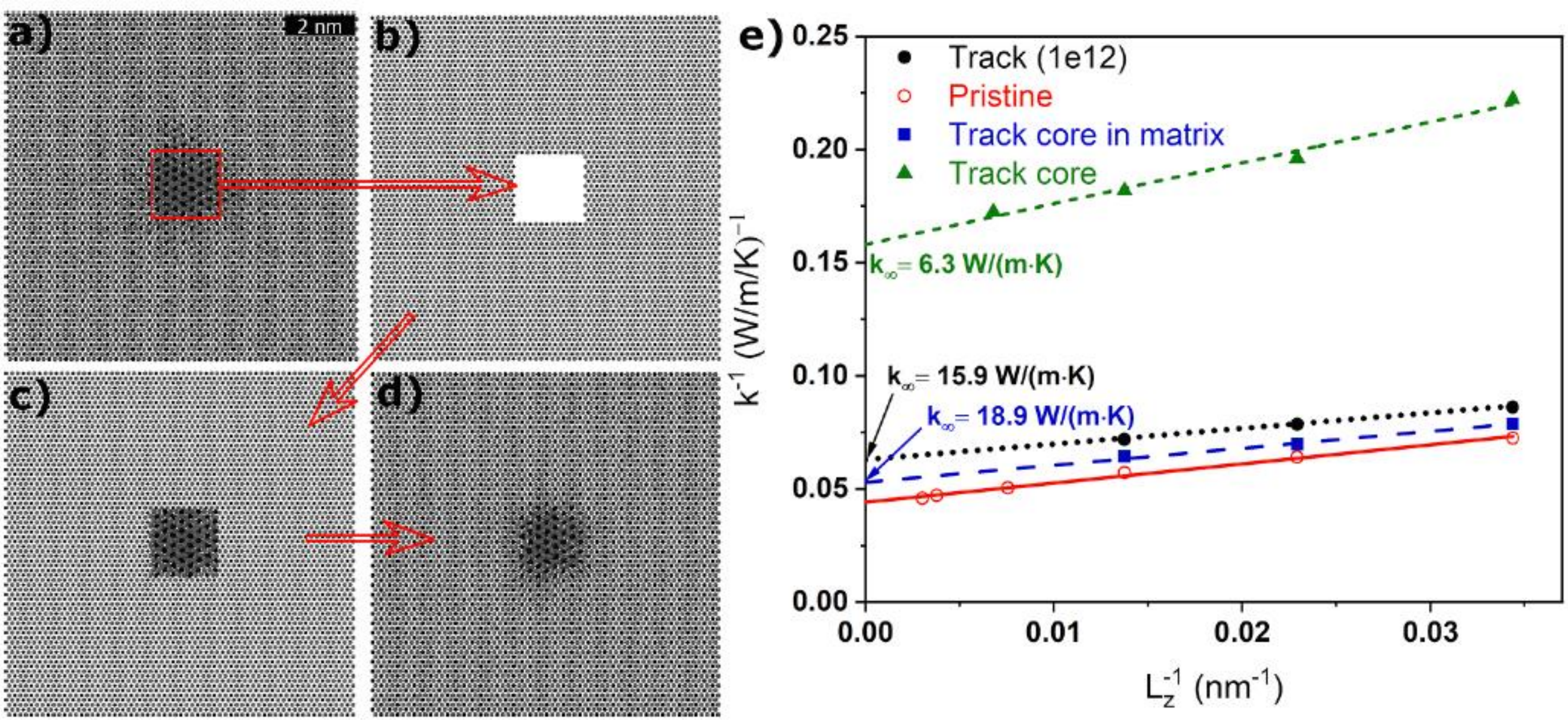

(a) MD image of 167 MeV Xe ion track in Al2O3. Red square shows the cut of the track core of 2×2 nm^2 in size; (b) pristine matrix and (c) track core inserted into pristine matrix in order to eliminate effects of track halo; (d) MD image of track core in pristine matrix relaxed at 300 K with NPT ensemble; (e) Finite-size scaling of calculated thermal conductivity (with linear fits) of MD cells shown in (a) and (d).

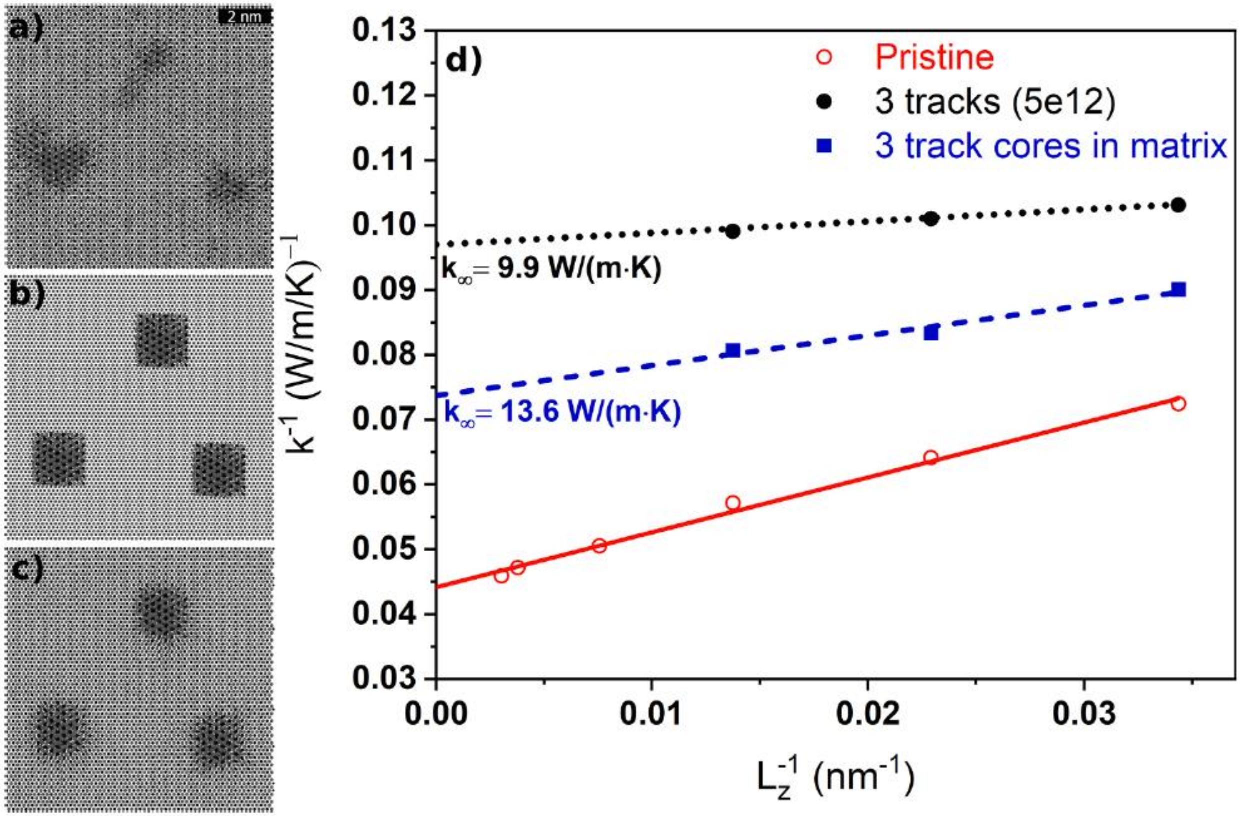

(a) MD image of three subsequent 167 MeV Xe tracks in Al2O3. (b) pristine matrix with inserted three track cores; (c) MD image of three track cores in pristine matrix relaxed at 300 K with NPT ensemble. (d) Finite-size scaling of calculated thermal conductivity (with linear fits) of MD cells shown in (a) and (c).

SUMMARY

- For the first time thermal transport was simulated in SHI irradiated solid using a direct method, which demonstrated good applicability in this case. Degradation of the thermal conductivity of single-crystalline Al2O3 with fluence demonstrates good agreement with the experimental TDTR data.

- The applied method allowed to separate an effect of discontinuous crystalline cylindrical tracks from that of an amorphous surface layer on the thermal conductivity of irradiated alumina. The results demonstrate that a very narrow highly damaged track core, created by SHI, most strongly affects the heat transport in such targets.

- The obtained data can be used for prediction of long-term radiation stability and thermal properties of materials exposed with fission fragments. They also can be used as the basis for the design of thermo-electronic devises with tailored properties and for advanced technologies of their productions.

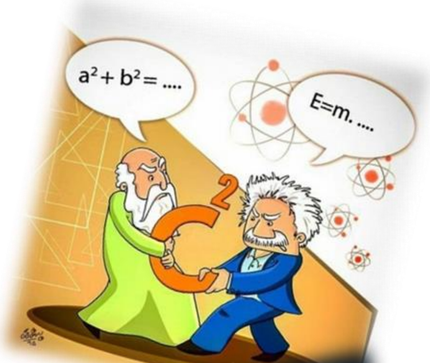


Electron: **goes through both slits**

Physicist: **places a detector**

Electron:

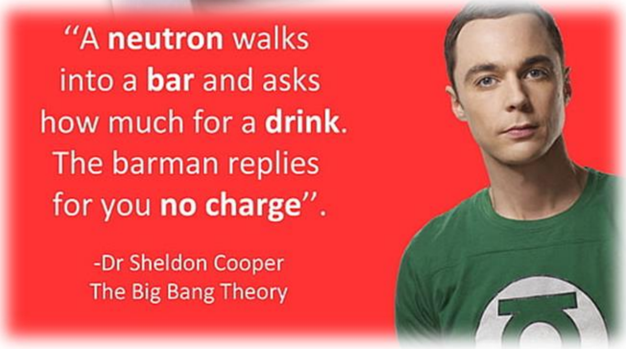
“A **neutron** walks into a **bar** and asks how much for a **drink**. The barman replies for you **no charge**”.

-Dr Sheldon Cooper
The Big Bang Theory

Thank you for attention!

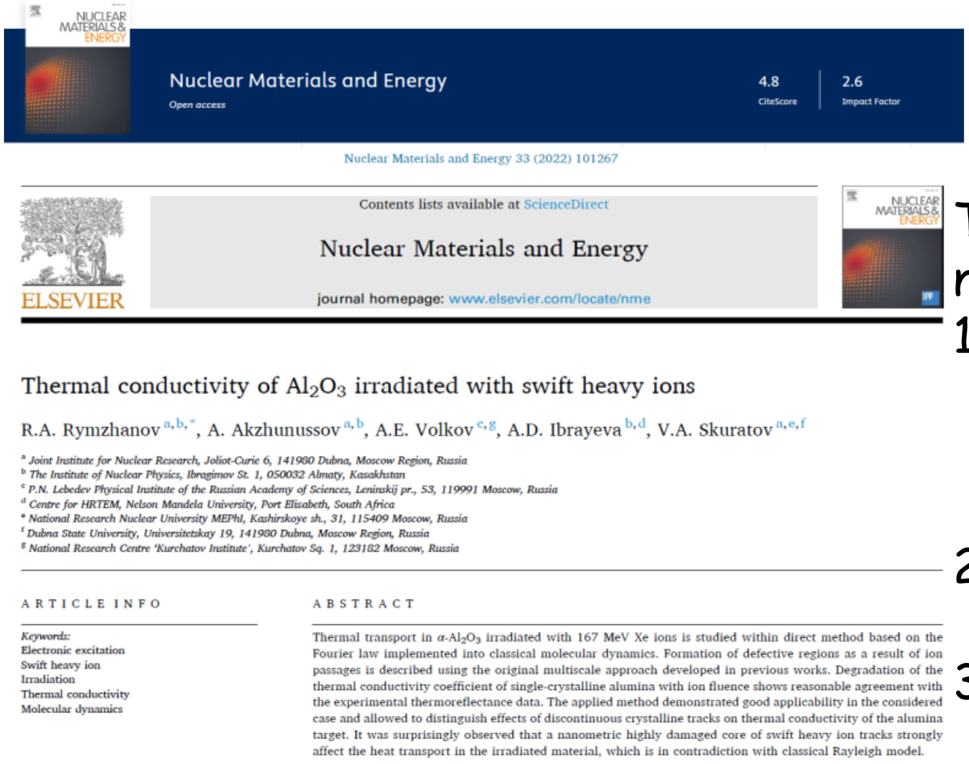

Nuclear Materials and Energy

Open access

4.8 CiteScore | 2.6 Impact Factor

Nuclear Materials and Energy 33 (2022) 101267

Contents lists available at ScienceDirect

Nuclear Materials and Energy

journal homepage: www.elsevier.com/locate/nme

Thermal conductivity of Al_2O_3 irradiated with swift heavy ions

R.A. Rymzhanov[a,b,*], A. Akzhunussov[a,b], A.E. Volkov[c,g], A.D. Ibrayeva[b,d], V.A. Skuratov[a,e,f]

[a] *Joint Institute for Nuclear Research, Joliot-Curie 6, 141980 Dubna, Moscow Region, Russia*
[b] *The Institute of Nuclear Physics, Ibragimov St. 1, 050032 Almaty, Kasakhstan*
[c] *P.N. Lebedev Physical Institute of the Russian Academy of Sciences, Leninskij pr., 53, 119991 Moscow, Russia*
[d] *Centre for HRTEM, Nelson Mandela University, Port Elisabeth, South Africa*
[e] *National Research Nuclear University MEPhI, Kashirskoye sh., 31, 115409 Moscow, Russia*
[f] *Dubna State University, Universitetskay 19, 141980 Dubna, Moscow Region, Russia*
[g] *National Research Centre 'Kurchatov Institute', Kurchatov Sq. 1, 123182 Moscow, Russia*

ARTICLE INFO

Keywords:
Electronic excitation
Swift heavy ion
Irradiation
Thermal conductivity
Molecular dynamics

ABSTRACT

Thermal transport in α-Al_2O_3 irradiated with 167 MeV Xe ions is studied within direct method based on the Fourier law implemented into classical molecular dynamics. Formation of defective regions as a result of ion passages is described using the original multiscale approach developed in previous works. Degradation of the thermal conductivity coefficient of single-crystalline alumina with ion fluence shows reasonable agreement with the experimental thermoreflectance data. The applied method demonstrated good applicability in the considered case and allowed to distinguish effects of discontinuous crystalline tracks on thermal conductivity of the alumina target. It was surprisingly observed that a nanometric highly damaged core of swift heavy ion tracks strongly affect the heat transport in the irradiated material, which is in contradiction with classical Rayleigh model.

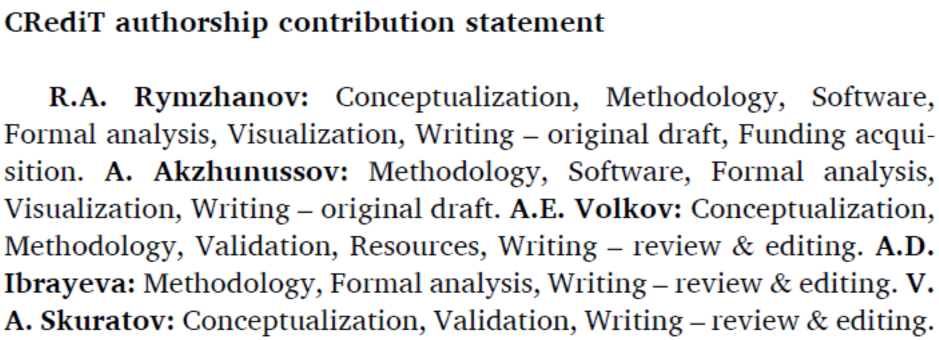

CRediT authorship contribution statement

R.A. Rymzhanov: Conceptualization, Methodology, Software, Formal analysis, Visualization, Writing – original draft, Funding acquisition. **A. Akzhunussov:** Methodology, Software, Formal analysis, Visualization, Writing – original draft. **A.E. Volkov:** Conceptualization, Methodology, Validation, Resources, Writing – review & editing. **A.D. Ibrayeva:** Methodology, Formal analysis, Writing – review & editing. **V. A. Skuratov:** Conceptualization, Validation, Writing – review & editing.

Materials Science (miscellaneous) 2022 Q1

Acknowledgement

This work has been carried out using next computing resources:

1) Federal collective usage center Complex for Simulation and Data Processing for Mega-science Facilities at NRC "Kurchatov Institute"
2) GSI Helmholtzzentrum (Darmstadt, Germany)
3) HybriLIT heterogeneous computing platform (LIT, JINR)

hYBRI LIT/JINR

Appendix_1: Interatomic potential

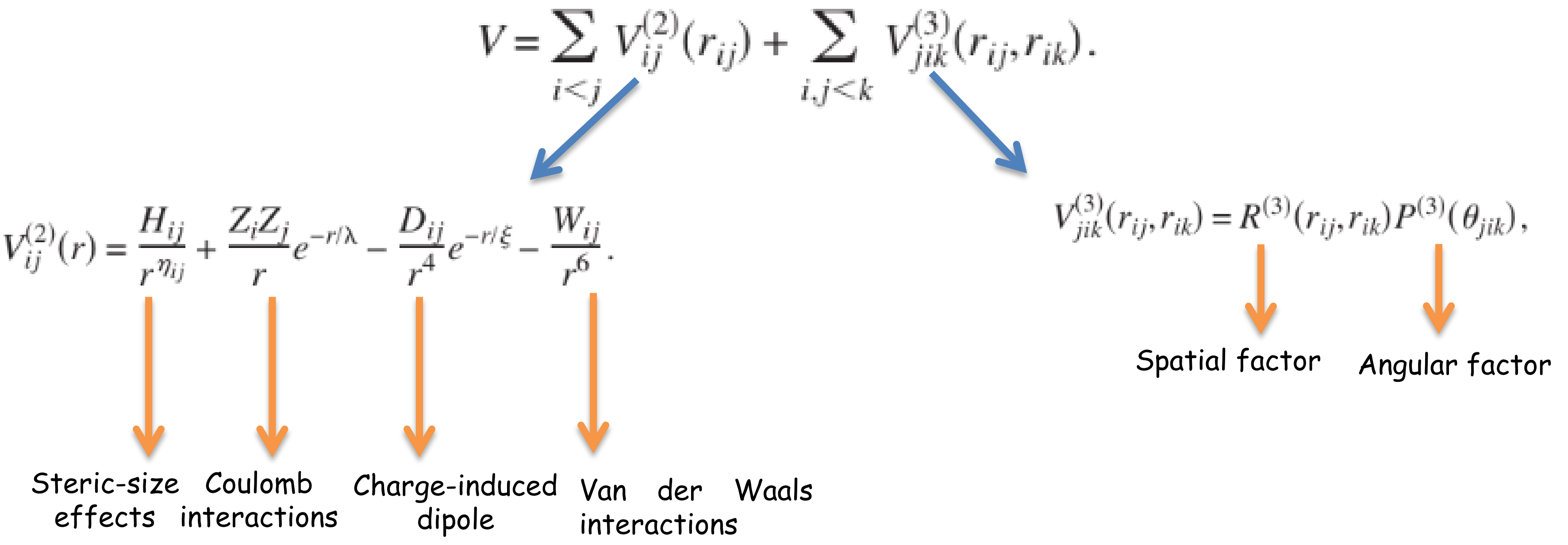

$$V = \sum_{i<j} V_{ij}^{(2)}(r_{ij}) + \sum_{i,j<k} V_{jik}^{(3)}(r_{ij}, r_{ik}).$$

$$V_{ij}^{(2)}(r) = \frac{H_{ij}}{r^{\eta_{ij}}} + \frac{Z_i Z_j}{r} e^{-r/\lambda} - \frac{D_{ij}}{r^4} e^{-r/\xi} - \frac{W_{ij}}{r^6}.$$

Steric-size effects

Coulomb interactions

Charge-induced dipole

Van der Waals interactions

$$V_{jik}^{(3)}(r_{ij}, r_{ik}) = R^{(3)}(r_{ij}, r_{ik}) P^{(3)}(\theta_{jik}),$$

Spatial factor

Angular factor

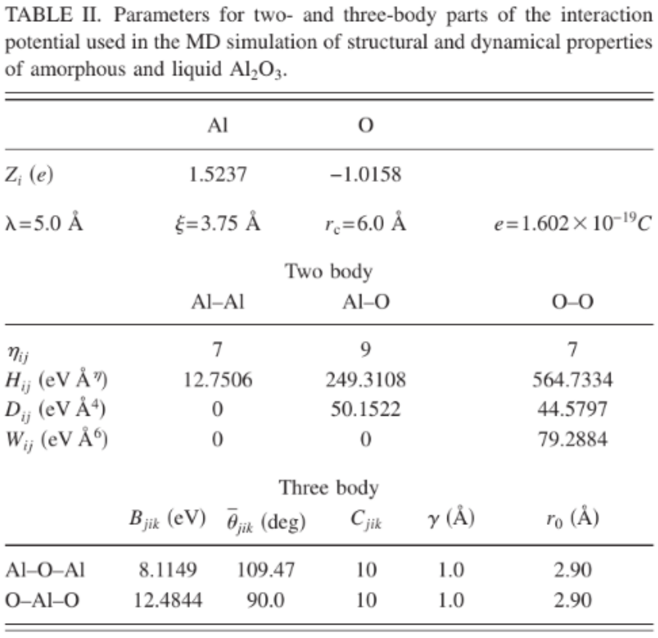

TABLE II. Parameters for two- and three-body parts of the interaction potential used in the MD simulation of structural and dynamical properties of amorphous and liquid Al_2O_3.

	Al	O			
Z_i (e)	1.5237	−1.0158			
$\lambda=5.0$ Å	$\xi=3.75$ Å	$r_c=6.0$ Å			$e=1.602\times10^{-19}C$
		Two body			
	Al–Al	Al–O			O–O
η_{ij}	7	9			7
H_{ij} (eV Å$^{\eta}$)	12.7506	249.3108			564.7334
D_{ij} (eV Å^4)	0	50.1522			44.5797
W_{ij} (eV Å^6)	0	0			79.2884
		Three body			
	B_{jik} (eV)	$\bar{\theta}_{jik}$ (deg)	C_{jik}	γ (Å)	r_0 (Å)
Al–O–Al	8.1149	109.47	10	1.0	2.90
O–Al–O	12.4844	90.0	10	1.0	2.90

From paper

Interaction potentials for alumina and molecular dynamics simulations of amorphous and liquid alumina

Priya Vashishta, Rajiv K. Kalia, Aiichiro Nakano and José Pedro Rino

JOURNAL OF APPLIED PHYSICS 103, 083504v (2008)

https://doi.org/10.1063/1.2901171

Appendix 2:TREKIS and MD

Time-Resolved Electron Kinetics in SHI Irradiated Solids

Collective response of a material is taken into account

(a) passage of a swift heavy ion ionizing the target and generating primary electrons and holes;
(b) interaction of δ-electrons with lattice and target electrons and further secondary electronic cascades;
(c) Auger decays of deep shell holes also producing secondary electrons;
(d) Radiative decays of core holes, following photon transport and photoabsorption exciting new electrons and holes;
(e) Valence, holes redistribution and their interaction with electrons and lattice

The dynamic structure factor - complex dielectric function formalism is applied to build up cross sections describing charged particles interactions within TREKIS.

$$\frac{d^2\sigma}{d(\hbar\omega)d(\hbar q)} = \underbrace{\boxed{\frac{2[Z_e(v,q)e]^2}{\pi\hbar^2 v^2}\frac{1}{\hbar q}}}_{\textit{Scattering center}} \underbrace{\boxed{\mathrm{Im}\left[\frac{-1}{\varepsilon(\omega,q)}\right]}}_{\textit{Loss function}},$$

From paper

Time-resolved electron kinetics in swift heavy ion irradiated solids

N A Medvedev, R A Rymzhanov and A E Volkov

J. Phys. D: Appl. Phys. 48 (2015) 355303 (24pp)

http://dx.doi.org/10.1088/0022-3727/48/35/355303

Appendix_3: Direct method TC

$$\left.\begin{aligned}
&\frac{1}{l_{\mathrm{eff}}}=\frac{1}{l_\infty}+\frac{4}{L_z}.\\[2ex]
&\kappa=\tfrac{1}{3}\ \mathrm{cvl},\\[2ex]
&c=\tfrac{3}{2}k_B n,
\end{aligned}\right\}\ \frac{1}{\kappa}=\frac{a^3}{4k_B v}\left(\frac{1}{l_\infty}+\frac{4}{L_z}\right).$$

From paper

Comparison of atomic-level simulation methods for computing thermal conductivity

Patrick K. Schelling, Simon R. Phillpot, and Pawel Keblinski

PHYSICAL REVIEW B, VOLUME 65, 144306

https://doi.org/10.1103/PhysRevB.65.144306

Appendix_4: Experimental details of TC

Picosecond time domain thermoreflectance (TDTR)

To perform near surface nanoscale thermal transport measurement on irradiated sapphire samples, have implemented the TDTR setup. The Ti:Al2O3 mode-locked femtosecond laser (Tsunami, Spectra Physics) at 782 nm wavelength, 80 MHz repetition rate and 80 fs pulse duration, was used as pump and probe beams.

Recorded picosecond TDTR signal of $-V_{in}/V_{out}$ as a function of delay time between pump and probe beams was fitted with a thermal diffusion model to extract unknown thermal conductivity. The thermal analysis was based on the iterative algorithm applied to a multilayer geometry with thermal conductivity, volumetric specific heat capacity, and thickness defined for each layer.

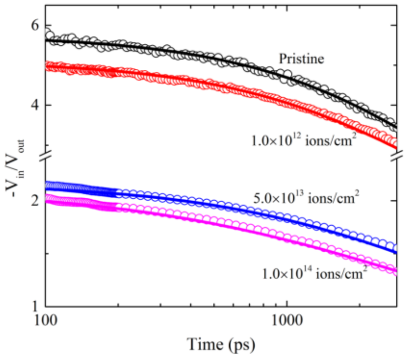

Fluence (ions/ cm^2)	$k_{ion\ track\ layer}$ (W/m K) measured by TDTR
Pristine	31.2 ± 4.8
1.0×10^{12}	14.5 ± 2.3
5.0×10^{13}	5.8 ± 0.7
1.0×10^{14}	4.8 ± 0.7

From paper

Thermal transport across nanoscale damage profile in sapphire irradiated by swift heavy ions

A. Abdullaev, V. S. Chauhan, B. Muminov, J. O'Connell, V. A. Skuratov, M. Khafizov and Z. N. Utegulov

J. Appl. Phys. 127, 035108 (2020)

https://doi.org/10.1063/1.5126413

CW Millenia pumped Tsunami femtosecond laser for ultrafast thermoreflectance studies